JOC The Journal of Organic Chemistry

Note

pubs.acs.org/joc

2,3-Naphtho-Fused BODIPYs as Near-Infrared Absorbing Dyes

Sho Yamazawa, Mika Nakashima, Yukie Suda, Ryuhei Nishiyabu, and Yuji Kubo*

Department of Applied Chemistry, Graduate School of Urban Environmental Sciences, Tokyo Metropolitan University, 1-1 Minami-Ohsawa, Hachioji, Tokyo 192-0397, Japan

Supporting Information

ABSTRACT: 2,3-Naphtho-fused boron-dipyrromethenes (BODIPYs) **1a** and **1b**, which absorb near-infrared light at 740−770 nm with molar extinction coefficients above 10^5 M^{-1} cm^{-1} in THF, have been synthesized through a palladium(II)-catalyzed direct acylation of *N*-BOC hydrazones and subsequent Paal−Knorr pyrrole synthesis. Simple benzo-annulation of dibenzo-BODIPY caused a significant red-shift in the absorption. Subsequent intramolecular *B*,*O*-cyclization of **1b** gave **2**, which exhibited an intense absorption band at 830 nm. The structure−optical property relationship has been investigated using theoretical calculations and cyclic voltammetry.

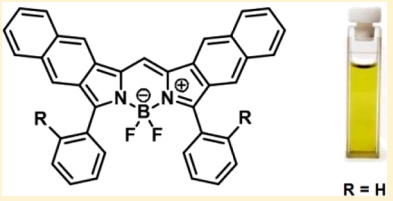

Intense demand for efficient photosensitizers for organic solar cells[1] and for biological applications, such as photodynamic therapy[2] and bioimaging,[3] have motivated us to synthesize near-infrared (NIR) absorbing dyes with high molar extinction coefficients (ε) in this wavelength region.[4] The synthesis and characterization of NIR dyes have emerged as a major research field over the past few decades with polymethine dyes,[5] quinones,[6] azo compounds,[7] phthalocyanines,[8] and bisanthenes[9] attracting particular interest. In this context, their application requires robust dyes with synthetic diversity.

Boron complexes with dipyrrin cores, the so-called BODIPY dyes, have emerged as promising candidates because of their outstanding optical properties, such as high ε values of absorption, high fluorescence quantum yields, and excellent photostability.[10] In particular, facile structure modification of the BODIPY core has allowed preparation of BODIPY- and aza-BODIPY-based NIR dyes through extension of the π-conjugation framework.[11] Among the strategies to shift the absorption of BODIPYs to longer wavelengths, π-extension by fusing aromatic units to the *a*-bond or *b*-bond of the pyrrole moiety is particularly promising (Figure 1). Since the first example of a benzo-[*a*]-fused BODIPY was prepared by Kang and Haugland,[12] many related derivatives have been synthesized and characterized. Although such a dye core itself cannot absorb NIR light,[13] synthetic modification based on the insertion of electron-donor thiophene units into the core[13d,e] and the formation of benzo[1,3,2]oxazaborinine-based intramolecular *B*,*O*-chelates led to the production of related NIR dyes.[14] Alternatively, π-extension at the [*b*] bond position has led to furan-[15] and thiophene-fused[16] NIR dyes. In line with this strategy, synthesis of highly annulated BODIPY species is an attractive research target.[17] To date, not only have phenanthrene,[18] naphthobipyrrole,[19] and acenaphthylene-fused[20] NIR BODIPYs been reported, but also fused bis(BODIPY) derivatives.[21] However, given the easy-to-understand aromatic π-extension effect on the absorption and florescence spectra of such dyes, simple linearly annulated BODIPYs, such as 2,3-naphtho-[*a*]-fused BODIPY, are an intriguing prospect. However, such dyes have not been prepared yet, perhaps because [*a*]-fused BODIPY has a lower stability than [*b*]-fused BODIPY.[22] Indeed, isolation of 2,3-naphtho-[*a*]-fused aza-BODIPY **A** (Figure 1) has been unsuccessful.[23]

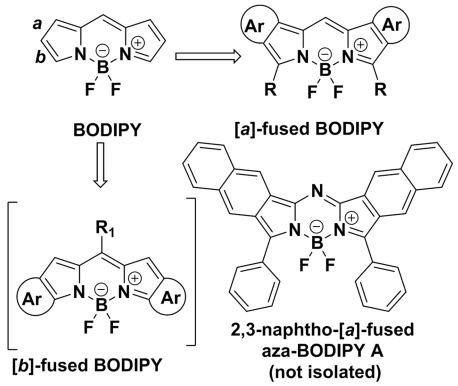

Figure 1. Aromatic ring-fused BODIPY derivatives and aza-analogues.

In this Note, we report that dyes **1a** and **1b**, which show an intense absorption band in the NIR region with ε values of $>10^5$ M^{-1} cm^{-1} in THF, have been successfully synthesized for the first time. Furthermore, intramolecular *B*,*O*-ring formation of **1b** with BBr_3 allowed us to prepare the related benzo-[1,3,2]oxazaborinine dye **2**, which can absorb NIR light beyond 800 nm. Their optical properties have been discussed using theoretical calculations and cyclic voltammetry (CV).

The synthetic path is shown in Scheme 1. The palladium(II)-catalyzed direct acylation[24] of *tert*-butyl *N*-(1-naphthalen-2-yletyleneamino)carbamate **3**[25] with **4a** afforded 1,2-diacylbenzene **5a**[24] through C−H activation. The subsequent Paal−Knorr pyrrole synthesis gave naphthalene-fused dipyrrin **6a** in

Received: November 29, 2015
Published: January 6, 2016

DOI: 10.1021/acs.joc.5b02720
J. Org. Chem. 2016, 81, 1310−1315

Scheme 1. Synthesis of 2,3-Naphtho-Fused BODIPYs

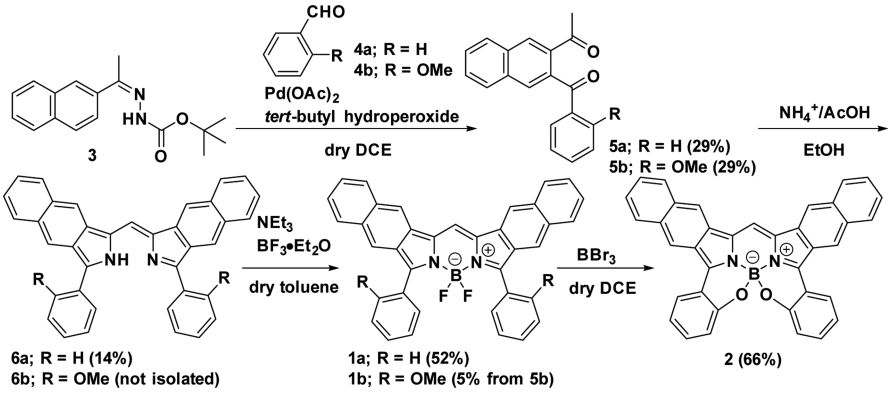

14% yield, although it was somewhat unstable in solution. BF_2-chelation of **6a** using $BF_3{\cdot}Et_2O$ afforded **1a** in 52% yield. Synthesis of anisole derivative **1b** was attempted via a similar procedure, where it was found that the color of the TLC spot assignable to **6b** gradually changed, possibly due to the enhanced instability of the electron-donating anisole-attached 2*H*-benzo[*f*]isoindole intermediate generated in the Paal–Knorr reaction. Accordingly, **1b** was prepared from **5b** through sequential two-step reactions without isolating **6b** (see Experimental section). Subsequent intramolecular *B*,*O*-cyclization of **1b** with BBr_3 gave **2** in 66% yield.

The target NIR dyes were assigned on the basis of spectroscopic analysis involving NMR, mass spectroscopy, and elemental analysis. In the ^{13}C NMR of **1a** and **1b**, the signals assignable to the *β*-carbon atoms of the phenyl groups at the 3-positions of the 2*H*-benzo[*f*]isoindole moiety appear as well-resolved triplets at 131.3 ppm (J = 2.94 Hz) and 133.3 ppm (J = 3.38 Hz). These carbon atoms are involved in intramolecular C–H···F interactions.[13f,26] A crystal of **1a** suitable for X-ray diffraction analysis was successfully obtained, and the structure is shown to belong to the monoclinic $P2_1/n$ space group (Figure 2a). The average root-mean-square deviation of the di(naphtho)-fused diazaindacene is 0.098 Å, indicating that **1a** adopts an almost planar *π*-conjugation conformation. In contrast, phenyl rings at the 3- and 3′-positions of the 2*H*-benzo[*f*]isoindole are tilted by 40°–50° relative to the naphtho-fused BODIPY core. The C–F distances were estimated to be 2.397 and 2.251 Å (Figure 2b), which were smaller than the sum of the van der Waals radii for hydrogen and fluorine (2.62 Å).[26b] This suggests the presence of an intramolecular interaction between the *ortho* proton in the phenyl ring and the fluorine of BF_2 (vide supra). The crystal packing diagram in Figure S1 showed that two neighboring molecules form *π*-stacked dimer structures in a head-to-tail arrangement with an intermolecular distance of 3.341 Å between the *π*-conjugated planes of the neighboring molecules, where the molecules are longitudinally arranged in a slightly offset fashion to avoid steric repulsion due to the phenyl ring at the 3-position of the 2*H*-benzo[*f*]isoindole ring. Figure 2c shows the columnar structure. Along the *b*-axis, the packing structure adopts a face-to-face alignment of the *π*-conjugated systems. Conversely, neighboring *π*-conjugated systems between stacked columns adopt an edge-to-face arrangement.

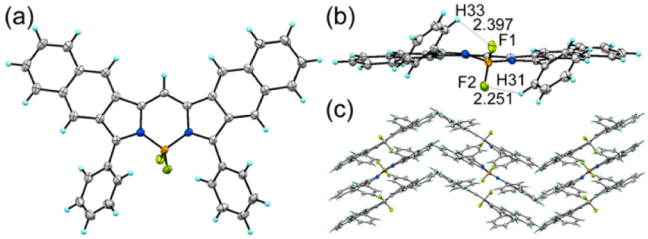

Figure 2. (a) X-ray crystal structure of **1a** where thermal ellipsoids are drawn at the 50% probably level, showing (b) the side view and (c) the packing structure.

The ^1H NMR spectrum of **1b** in DMSO-d_6 at 25 °C contains two sets of signals assignable to the anisole moiety with proton resonances arising from the methoxy groups being detected at 3.68 and 3.73 ppm, as shown in Figure S2. To further investigate this structure, we measured the ^{19}F NMR spectrum of **1b** in DMSO-d_6, which exhibited a quintet signal at −132.0 ppm (J_{BF} = 30.9 Hz) and apparent octet signals at −145.6 ppm (J_{BF} = 28.6 Hz, $^2J_{FF}$ = 95.8 Hz) and −120.0 ppm (J_{BF} = 33.0 Hz, $^2J_{FF}$ = 96.8 Hz), as shown in Figure S3. This indicates the presence of *anti*- and *syn*-isomers in which the anisole moieties are located on the opposite and same face of the diazaindacene core, respectively (Figure 3). To gain further insight into the structures, we recorded variable-temperature NMR spectra (Figure S2) of a DMSO-d_6 solution of **1b**, which revealed a T_c value of 105 °C ($\Delta G^{\#}$ = 80.7 kJ mol^{-1}). These results indicate that rotation about the two C–C bonds, which connect the anisole and 2*H*-benzo[*f*]isoindole ring, may be restricted.

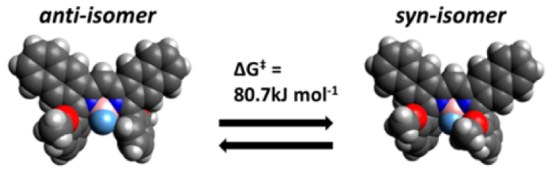

Figure 3. Proposed conformers of **1b**.

Figure 4 shows the absorption spectra of dyes obtained in this work and benzo-[*a*]-fused BODIPY **7**[13f] in THF at 25 °C; their spectral parameters are summarized in Table 1. Dye **1a** is yellow and absorbs NIR light at 761 nm with a relatively high *ε* value of 1.08 × 10^5 M^{-1} cm^{-1}. Note that a remarkable bathochromic shift of 121 nm compared to **7** was observed owing to simple benzo-annulation. Replacement of benzene with anisole at the 3-position of the 2*H*-benzo[*f*]isoindole ring led to the production of **1b** with a λ_{max} value of 738 nm (ε_{max} = 1.37 × 10^5 M^{-1} cm^{-1}). Despite the 23 nm hypsochromic shift

DOI: 10.1021/acs.joc.5b02720
J. Org. Chem. 2016, 81, 1310–1315

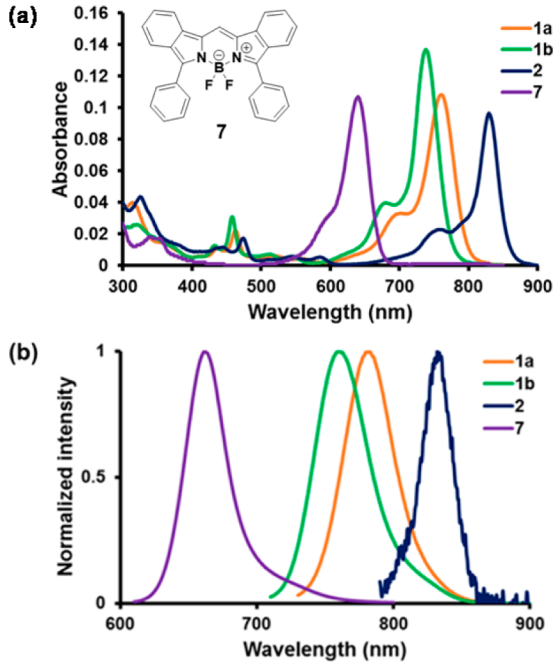

Figure 4. (a) Absorption and (b) fluorescence spectra of dyes (1 μM) in THF at 25 °C. λ_{ex} = 720 nm for **1a** and **2**, 700 nm for **1b**, and 600 nm for **7**.

Table 1. Absorption and Fluorescence Spectra of Dyes at 25 °C

dye	solvent	λ_{max} (nm)	ε^a	$\Delta\lambda^b$ (nm)	$\lambda_{em}{}^c$ (nm)	$\Delta_s{}^d$ (cm^{-1})	Φ_F (%)
1a	THF	761	1.08	121	782	353	16
	C_6H_6	765	1.13	125	785	333	21
	CH_2Cl_2	762	1.17	122	785	385	16
	DMF	764	1.00	124	788	399	14
1b	THF	738	1.37	98	760	392	29
2	THF	830	0.962	190	832	29	1.3
7	THF	640	1.07		662	519	57

[a]Molar extinction coefficient, in 10^5 M^{-1} cm^{-1}. [b]$\Delta\lambda = \lambda_{max} - \lambda_{max}$ of **7**. [c]λ_{ex} = 720 nm for **1a** and **2**. λ_{ex} = 700 nm for **1b**. λ_{ex} = 600 nm for **7**. [d]$\Delta_s = (1/\lambda_{max}) - (1/\lambda_{em})$.

relative to **1a**, an increase of 1.3 times in the ε value was observed, implying that additional substituents in the phenyl ring at the 3-position enables fine-tuning of the optical properties. We have found that **2** absorbs NIR light at a λ_{max} value of 830 nm in THF, showing a large bathochromic shift of 190 nm compared to that shown by **7**. This is due to the effective π-extension based on benzo-annulation and the immobilization of the coplanar conformation.

The fluorescence spectra were also measured in THF (Figure 4, Table 1). Dyes **1a** and **1b** emit NIR light with λ_{em} values of 782 and 760 nm, respectively, with a small Stokes shift (Δ_S = 350−400 cm^{-1}). This is possibly due to their rigid structure and is consistent with the trend observed for their absorption properties with π expansion based on ring fusion. Although these can serve as NIR fluorophores, the fluorescence quantum yields are much lower than that of **7**, which is ascribable to increased nonradiative deactivation as the energy gap decreases.[27] The solvent effect on the absorption and fluorescence spectra was investigated for **1a** (Figure S4), and almost no variation was observed with increasing polarity from benzene to DMF. However, the fluorescence quantum yield is slightly sensitive to the change in solvent polarity from benzene (Φ_F = 21%) to DMF (Φ_F = 14%). For **2**, a low fluorescence emission at 832 nm (Φ_F = 1.3%) was observed when excited at 720 nm. The very small Stokes shift value (29 cm^{-1}) suggests a conformationally restricted structure of **2**. Similar results were obtained for **1b** and **2** (Figures S5 and S6 and Table S1), although a low solubility of **2** against benzene did not allow the measurement.

For better understanding of these optical features, the transition energies were calculated using time-dependent density functional theory (TD-DFT) at the B3LYP/6-31G(d,p) level (Figure 5). The trend in the calculated λ_{max} of the longest

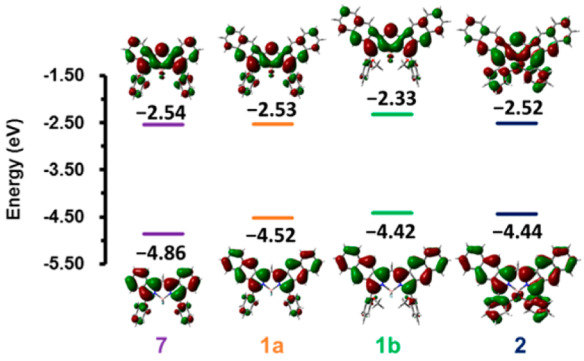

Figure 5. Energy diagram and surface plots of HOMO and LUMO energies of dyes (**7**, **1a**, **1b**, and **2**), as estimated from TD-DFT/DFT calculations (B3LYP/6-31G(d,p)).

absorption bands is almost consistent with that observed in the spectra recorded in THF (Table S2). Although the first absorption band was characterized as a mixture of several configurations, it can mainly be ascribed to the HOMO−LUMO transition. From **7** to **1a**, the calculation indicated an increase in the HOMO level from −4.86 to −4.52 eV, whereas the LUMO energy level remained unchanged. This led to a decrease in the HOMO−LUMO energy gap ($\Delta\Delta E$ = 0.33 eV). Note that the replacement of phenyl with anisole moieties at the 3-position (i.e., from **1a** to **1b**) led to destabilization of the HOMO and LUMO levels, where greater destabilization of the LUMO level of **1b** than that of the corresponding HOMO resulted in the hypthochromic shift of λ_{max} ($\Delta\lambda$ = 23 nm in THF; Table 1). Alternatively, intramolecular *B*,*O*-chelation resulted in the stabilization of both HOMO and LUMO levels compared to **1b**, where the LUMO level was found to be more stabilized by 0.17 eV than the HOMO level. Subsequently, a lower HOMO−LUMO energy gap was calculated for **2**, which induced a further bathochromic shift in the absorption band. The surface plots of both HOMO and LUMO levels were evaluated by DFT calculation and indicate that all of the HOMO and LUMO levels are homogeneously delocalized on the di(naphtho)diazaindacene core. As shown in Figure 5, the electron-density distribution on the naphthalene moiety for the HOMO level is stronger than that for the LUMO level, which is possibly responsible for the increase in HOMO energy upon benzo-annulation of **7**.

The electrochemical properties of **1a** and **1b** were measured at room temperature using CV in a CH_3CN/*o*-dichlorobenzene (2:3 v/v) mixture containing 0.1 M tetrabutylammonium hexafluorophosphate ($TBAPF_6$) as the supporting electrolyte. The low solubility of **2** in such organic solvents prevented its

DOI: 10.1021/acs.joc.5b02720
J. Org. Chem. 2016, 81, 1310−1315

CV analysis. The measurements were calibrated against ferrocene (−4.8 eV) as the standard.[28] The formal potential of Fc/Fc^+ was measured to be 0.06 V versus Ag/Ag^+. The cyclic voltammograms obtained for the dyes are illustrated with that of **7** in Figure S7. The reversible oxidation and reduction processes allowed us to determine the onset oxidation and reduction potentials corresponding to HOMO and LUMO energies, respectively (Table S3). When compared to those of **7**, we have found a significant increase of HOMO energy of **1a** (ΔE = 0.20 eV), whereas the LUMO energy level is almost the same, which is consistent with the calculated results. Accordingly, we confirmed that benzo-annulation with respect to **7** leads to an increase in the HOMO level. In addition, a hypsochromic shift in the longest-wavelength absorption band from **1a** to **1b** can be rationalized by a slight increase in the LUMO energy level (ΔE = 0.08 eV). In this way, the effect of ring expansion on the optical properties of the dyes has been evaluated.

In conclusion, NIR-absorbing 2,3-naphtho-[*a*]-fused BODIPY dyes have been synthesized for the first time. Interestingly, we found that linear benzo-annulation to dibenzo-[*a*]-fused BODIPY induced a remarkable red-shift of more than 100 nm owing to an increase in the HOMO level. It was also found that the optical properties were sensitive to the electronic nature of the phenyl unit at the 3-position of the 2*H*-benzo[*f*]isoindole ring despite the ring being tilted by 40°−50° relative to the di(naphtho)diazaindacene core. Replacement of benzene with anisole (i.e., from **1a** to **1b**) caused a blue-shift in the absorption with increasing ε values. Also, intramolecular *B*,*O*-chelation of **1b** was effective for tuning the LUMO level. Our analysis of the structure−optical property relationship indicated that even slight perturbation of the dye structure can cause an effective change in their optical features. We believe that these insights could contribute to the rational design of BODIPY-based NIR dyes for applications in material science involving organic photovoltaics.[29]

EXPERIMENTAL SECTION

General. NMR spectra were measured on a 500 MHz spectrometer (^{1}H: 500 MHz, ^{13}C: 125 MHz, ^{19}F: 470 MHz). In ^{1}H and ^{13}C NMR measurements, chemical shifts (δ) are reported downfield from the internal standard Me_4Si. In addition, fast atom bombardment (FAB) mass spectra were obtained where *m*-nitrobenzylalcohol was used as a matrix. Mass spectrometry data of **6a** and **2** were taken by using an atmospheric pressure chemical ionization (APCI) method. The absorption and fluorescence spectra were measured using UV−vis−NIR spectroscopy and a spectrofluorometer, respectively. Elemental analyses were performed on an Elemental Analyzer.

Materials. Reagents used for the synthesis were commercially available and used as supplied. Dry 1,2-dichloroethane and dry THF were prepared according to a standard procedure. *tert*-Butyl *N*-(1-naphthalen-2-yletyleneamino)carbamate **3**[25] was obtained by condensing 2-acetonaphthone with *tert*-butyl carbazate in 83% yield.

Synthesis. *1-(3-Benzoylnaphthalen-2-yl)ethanone (**5a**).*[24] To an autoclave with a solution of **3** (8.53 g, 30.0 mmol), $Pd(OAc)_2$ (0.68 g, 3.03 mmol), and benzaldehyde **4a** (9.1 mL, 90.0 mmol) in dry 1,2-dichloroethane (100 mL) was slowly added *tert*-butyl hydroperoxide (22 mL, 120 mmol, 5.0−6.0 M in decane). The reaction mixture was stirred at 70 °C for 6 h. After cooling, the solution was poured into saturated Na_2CO_3 aqueous solution and extracted with CH_2Cl_2. The resultant organic layer was washed with saturated Na_2CO_3 aqueous solution and water, dried with Na_2SO_4, and filtered. After removal of the solvent, the residue was chromatographed on silica gel (Wakogel C-300) using a gradient of CH_2Cl_2 (15−50%) in hexane. In this way, 2.37 g of **5a** was obtained in 29% yield. ^{1}H NMR (500 MHz,$CDCl_3$) δ (ppm): 8.39 (s, 1H), 8.02 (dd, 1H, *J* = 6.13 and 3.07 Hz), 7.90 (dd, 1H, *J* = 6.17 and 3.13 Hz), 7.87 (s, 1H), 7.80 (dt, 2H, *J* = 8.20 and 153 Hz), 7.64−7.70 (m, 2H), 7.55 (tt, 1H, *J* = 7.40 and 1.65 Hz), 7.41−7.44 (m, 2H), 2.64 (s, 3H). ^{13}C NMR (125 MHz, $CDCl_3$) δ (ppm): 198.3, 197.4, 137.6, 137.1, 135.7, 134.0, 132.8, 132.7, 130.9, 129.4, 129.3, 129.1, 128.7, 128.4, 128.4, 128.1, 27.3. HRMS (FAB) *m*/*z*: $[M + H]^+$ calcd for $C_{19}H_{15}O_2$, 275.1067; found, 275.1056.

*1-(3-(2-Methoxybenzoyl)naphthalen-2-yl)ethanone (**5b**).* To a sealed tube with a solution of **3** (1.41g, 4.95 mmol), *o*-anisalaldehyde **4b** (2.00g, 14.7 mmol), and $Pd(OAc)_2$ (0.12g, 0.534 mmol) in dry 1,2-dichloroethane (17 mL) was added *tert*-butyl hydroperoxide (3.6 mL, 19.8 mmol, 5.0−6.0 M in decane). The mixture was stirred overnight at 70 °C. After cooling, the resultant solution was poured into saturated Na_2CO_3 aqueous solution and partitioned with CH_2Cl_2/saturated NaCl aqueous solution. The organic solution was dried with Na_2SO_4 and evaporated. The residue was then chromatographed on silica gel (Wakogel C-300) using hexane/AcOEt (5:1 v/v) as an eluent. In this way, 0.447 g of **5b** was obtained in 29% yield. ^{1}H NMR (500 MHz, $CDCl_3$) δ (ppm): 8.15 (s, 1H), 7.95−7.97 (m, 1H), 7.83−7.85 (m, 2H), 7.71 (dd, 1H, *J* = 7.65 and 1.75 Hz), 7.62 (td, 1H, *J* = 6.06 and 1.77 Hz), 7.60 (td, 1H, *J* = 6.02 and 1.82 Hz), 7.51 (ddd, 1H, *J* = 8.70, 7.08, and 1.37 Hz), 7.05 (td, 1H, *J* = 7.53 and 0.80 Hz), 6.97 (d, 1H, *J* = 8.25 Hz), 3.63 (s, 3H), 2.59 (s, 3H). ^{13}C NMR (125 MHz, $CDCl_3$) δ (ppm): 200.5, 196.1, 158.7, 138.4, 137.3, 133.6, 133.6, 133.2, 131.3, 129.4, 128.9, 128.8, 128.7, 128.5, 128.2, 127.6, 120.6, 112.0, 55.7, 28.5. HRMS (FAB): *m*/*z* $[M + H]^+$ calcd for $C_{20}H_{17}O_3$, 305.1172; found, 305.1179.

*2,3-Naphtho-[a]-fused Dipyrrin (**6a**).* To a solution of **5a** (1.84 g, 6.71 mmol) and AcOH (14.5 mL) in EtOH (71.5 mL) were added NH_4OAc (3.22 g, 41.8 mmol) and NH_4Cl (0.375 g, 7.01 mmol) at 65 °C. The resulting solution was stirred at 90 °C for 3 h. After cooling, the resultant solution was neutralized with $NaHCO_3$ aqueous solution to give a precipitate followed by reprecipitation through diffusion of EtOH into the CH_2Cl_2 solution to afford **6a** as a dipyrrin analogue (225 mg) in 14% yield. ^{1}H NMR (500 MHz, $CDCl_3$) δ (ppm): 8.57 (s, 2H), 8.46 (s, 2H), 8.18 (d, 4H, *J* = 7.25 Hz), 7.97 (d, 2H, *J* = 7.65 Hz), 7.96 (d, 2H, *J* = 7.65 Hz), 7.81 (s, 1H), 7.63 (t, 4H, *J* = 7.73 Hz), 7.49 (t, 2H, *J* = 7.45 Hz), 7.45 (td, 2H, *J* = 8.04 and1.38 Hz), 7.39 (td, 2H, *J* = 7.33 and 1.10 Hz). ^{13}C NMR: not determined due to low stability. HRMS (APCI): *m*/*z* $[M]^+$ calcd for $C_{37}H_{24}N_2$, 496.1939; found, 496.1949.

*2,3-Naphtho-[a]-fused BODIPY (**1a**).* Dipyrrine **6a** (0.225 g, 0.453 mmol) was dissolved in dry toluene (18 mL) at 80 °C. To the solution was added NEt_3 (0.2 mL) and BF_3-Et_2O (1.0 mL, 7.96 mmol). The resulting solution was stirred overnight at 100 °C. After cooling and quenching with water, the residue was partitioned between CH_2Cl_2 and water. The organic layer was then dried with Na_2SO_4 and filtered off. After evaporation of the filtrate, the residue was chromatographed on silica gel (Wakogel C-300) using a gradient of CH_2Cl_2 (30−67%) in hexane as an eluent. In this way, **1a** (129 mg) was obtained in 52% yield. ^{1}H NMR (500 MHz, $CDCl_3$) δ (ppm): 8.46 (s, 2H), 8.20 (s, 2H), 8.05 (s,1H), 7.97 (d, 2H, *J* = 8.65 Hz), 7.93 (d, 4H, *J* = 7.10 Hz), 7.85 (d, 2H, *J* = 8.35 Hz), 7.57 (t, 4H, *J* = 7.22 Hz), 7.53 (t, 2H, *J* = 7.18 Hz), 7.46 (t, 2H, *J* = 7.40 Hz), 7.36 (t, 2H, *J* = 7.20 Hz). ^{13}C NMR (125 Hz, THF-d_8) δ (ppm): 151.4, 135.1, 133.0, 132.4, 131.3 (t, *J* = 2.94 Hz), 130.6, 130.1, 129.4, 129.0, 127.8, 127.6, 125.8, 124.0, 118.1, 112.6. FAB-MS: *m*/*z* = 544 $[M]^+$. Elemental analysis for $C_{37}H_{23}BF_2N_2$: C, 81.63; H, 4.26; N, 5.15. Found: C, 81.48; H, 4.30; N, 5.18.

*Anisole-Derived Dye (**1b**).* Compound **5b** (0.404 g, 1.33 mmol) was dissolved in degassed EtOH (14 mL) and AcOH (4.4 mL) in a sealed tube under a N_2 atmosphere. To the solution was added 28% NH_3 aqueous solution (5.6 mL) with the resulting solution stirred at 85 °C for 5 h. The reaction mixture was quenched with water (100 mL) and extracted with CH_2Cl_2. The organic layer was dried with Na_2SO_4 and filtered off. After evaporation of the filtrate, a dark green solid (0.382 g) was obtained and dissolved in dry toluene (20 mL), which was degassed by freeze−pump−thaw cycle. To the solution at 80 °C were added NEt_3 (0.25 mL, 1.77 mmol) and BF_3-Et_2O (0.83 mL, 6.57 mmol). The resulting solution was stirred at 100 °C for 2.5 h.

DOI: 10.1021/acs.joc.5b02720
J. Org. Chem. 2016, 81, 1310−1315

The reaction mixture was quenched with water (100 mL) and partitioned between CH_2Cl_2 and water. The organic layer was dried with Na_2SO_4 and filtered off. After evaporation, the residue was chromatographed on silica gel (Wakogel C-300) using hexane/benzene (1:4 v/v) as an eluent, being followed by reprecipitation through diffusion of MeOH into the CH_2Cl_2 solution to afford **1b** (20.3 mg) as a conformation mixture ($\Delta G^{\#}$ = 80.7 kJ mol^{-1}) in 5% yield. ^{1}H NMR (500 MHz, DMSO-d_6, 25 °C) δ (ppm): 8.76 (s, 1H), 8.74 (s, 2H), 8.05 (d, 2H, J = 8.50 Hz), 8.03 (s, 2H), 8.01 (d, 2H, J = 9.15 Hz), 7.50−7.56 (m, 5H), 7.46 (d, 1H, J = 7.40 Hz), 7.38−7.41 (m, 2H), 7.27 (d, 1H, J = 8.05 Hz), 7.24 (d, 1H, J = 8.10 Hz), 7.12 (td, 1H, J = 7.50 and 0.88 Hz), 7.07 (td, 1H, J = 7.52 and 0.93 Hz), 3.73 (s, 3H), 3.68 (s, 3H). ^{13}C NMR (125 MHz, THF-d_8, 25 °C) δ (ppm): 159.3, 159.2, 149.6, 149.4, 135.0, 133.3 (t, J = 3.38 Hz), 132.9, 132.9, 132.5, 132.1, 132.0, 131.6, 131.5,130.5, 131.3, 130.5, 129.4, 127.2, 125.4, 123.9, 123.8, 121.6, 121.4,120.8, 120.7, 117.6, 112.7,112.7, 112.1, 112.0, 111.9, 55. 9, 55.8. ^{19}F NMR (470 MHz, DMSO-d_6, 25 °C) δ (ppm): −120.0 (octet, J_{BF} = 33.0 Hz, $^2J_{FF}$ = 96.8 Hz), −132.0 (quintet, J_{BF} = 30.9 Hz), −145.6 (octet, J_{BF} = 28.6 Hz, $^2J_{FF}$ = 95.8 Hz). FAB-MS: m/z = 604 $[M]^+$. Elemental analysis for $C_{39}H_{27}BF_2N_2O_2 \cdot 0.04CH_2Cl_2$: C, 77.14; H, 4.49; N, 4.61. Found: C, 76.94; H, 4.42; N, 4.65.

*Synthesis of Benzo[1,3,2]oxazaborinine Dye (**2**).* To the solution of **1b** (46 mg, 0.076 mmol) in dry 1,2-dichloroethane (7.6 mL) was added 1 M BBr_3 dichloromethane (0.4 mL) under icy conditions. The reaction mixture was stirred at 40 °C overnight. After quenching with sat. $NaHCO_3$ aqueous solution, the resulting organic solution was evaporated, precipitated with MeOH, and washed with acetone to give **2** (27 mg) in 66% as a moss green solid. ^{1}H NMR (500 MHz, DMSO-d_6) δ (ppm): 9.13 (s, 2H), 8.82 (s, 2H), 8.63 (dd, 2H, J = 7.82, 1.53 Hz), 8.49 (s, 1H), 8.20−8.23 (m, 2H), 8.09−8.11 (m, 2H), 7.56−7.59 (m, 2H), 7.50−7.54 (m, 2H), 7.43−7.48 (m, 2H), 7.30 (td, 2H, J = 7.55 and 1.18 Hz), 6.94 (dd, 2H, J = 8.45 and 0.85 Hz). ^{13}C NMR: not determined due to low solubility. HRMS (APCI) m/z: $[M + H]^+$ calcd for $C_{37}H_{22}BN_2O_2$, 537.1775; found 537.1799. Elemental analysis for $C_{37}H_{21}BN_2O_2 \cdot 0.5H_2O$: C, 81.48; H, 4.07; N, 5.14. Found: C, 81.64; H, 3.93; N, 5.17.

*X-ray Crystallography for **1a**.* A brown needle crystal of **1a** having approximate dimensions of 0.570 × 0.060 × 0.040 mm was mounted on a glass fiber. All measurements were made on an X-ray diffractometer using multilayer mirror monochromated Mo Kα radiation (λ = 0.71075 Å). The structure was solved by direct methods (SHELXS2013)[30] and expanded using Fourier techniques. The non-hydrogen atoms were refined anisotropically. Hydrogen atoms were refined using the riding model. The refinement was made by using a full-matrix least-squares technique (SHELXL2013).

The Measurement of Fluorescence Quantum Yield. The fluorescence quantum yields (Φ_{exp}) were calculated from eq 1.[31]

$$\Phi_{exp} = \Phi_R \times \frac{\int_0^\infty F(\lambda)\,d\lambda}{\int_0^\infty F_R(\lambda)\,d\lambda} \times \frac{A_R}{A} \times \frac{n^2}{{n_R}^2} \quad (1)$$

where $F(\lambda)$ and $F_R(\lambda)$ describe the corrected fluorescence intensities of the compound and the reference, respectively, and A and A_R describe the corresponding absorbance at the excitation wavelength. The reference used was indocyanine green (Φ_R = 0.12 in DMSO).[32]

Electrochemistry. Cyclic voltammograms (CV) were recorded on a potentiostat operated at a scan rate of 100 mV s^{-1} and room temperature under a N_2 atmosphere. The solvent was acetonitrile with *o*-dichlorobenzene (2:3 v/v) containing 0.1 M tetrabutylammonium hexafluorophosphate ($TBAPF_6$) as the supporting electrolyte. The potentials were measured against Ag/Ag$^+$ (0.01 M of $AgNO_3$) as a reference electrode; ferrocene/ferrocenium (Fc/Fc^+) was used as the internal standard and measured to be 0.06 V under the same conditions. The onset potentials were determined from the intersection of two tangents drawn at the rising and background currents of the cyclic voltammogram.

Theoretical Calculations. All geometries of the dyes at the ground state were fully optimized by means of the B3LYP/6-31G(d,p) level method. Density functional theory (DFT) calculations at the B3LYP/6-31G(d,p) level were performed in the Gaussian 09 package.[33] These molecular orbitals in Figure 5 were visualized using the Gauss view 5.0.8 program.

■ ASSOCIATED CONTENT

Supporting Information

The Supporting Information is available free of charge on the ACS Publications website at DOI: 10.1021/acs.joc.5b02720.

Additional crystal structure and spectroscopic data, characterization data for synthesized compounds, detailed single crystal X-ray diffraction study, and calculation results (PDF)

Crystallographic data for **1a** (CIF)

■ AUTHOR INFORMATION

Corresponding Author

*E-mail: yujik@tmu.ac.jp.

Notes

The authors declare no competing financial interest.

■ ACKNOWLEDGMENTS

This research was supported by JSPS KAKENHI Grant Number 26620033.

■ REFERENCES

(1) (a) Zhou, H.; Yang, L.; You, W. *Macromolecules* **2012**, *45*, 607−632. (b) Ragoussi, M.-E.; Torres, T. *Chem. Commun.* **2015**, *51*, 3957−3972. (c) Lee, C.-P.; Lin, R. Y.-Y.; Lin, L.-Y.; Li, C.-T.; Chu, T.-C.; Sun, S.-S.; Lin, J. T.; Ho, K.-C. *RSC Adv.* **2015**, *5*, 23810−23825.

(2) Kamkaew, A.; Lim, S. H.; Lee, H. B.; Kiew, L. V.; Chung, L. Y.; Burgess, K. *Chem. Soc. Rev.* **2013**, *42*, 77−88.

(3) Escobedo, J. O.; Rusin, O.; Lim, S.; Strongin, R. M. *Curr. Opin. Chem. Biol.* **2010**, *14*, 64−70.

(4) (a) Fabian, J.; Zahradnik, R. *Angew. Chem., Int. Ed. Engl.* **1989**, *28*, 677−694. (b) *Infrared Absorbing Dyes*; Matsuoka, M., Ed.; Plenum: New York, NY, 1990. (c) Fabian, J.; Nakazumi, H.; Matsuoka, M. *Chem. Rev.* **1992**, *92*, 1197−1226. (d) Qian, G.; Wang, Z. Y. *Chem. - Asian J.* **2010**, *5*, 1006−1029.

(5) Bricks, J. L.; Kachkovskii, A. D.; Slominskii, Y. L.; Gerasov, A. O.; Popov, S. V. *Dyes Pigm.* **2015**, *121*, 238−255.

(6) Kubo, Y.; Yoshida, K.; Adachi, M.; Nakamura, S.; Maeda, S. *J. Am. Chem. Soc.* **1991**, *113*, 2868−2873.

(7) Li, Y.; Patrick, B. O.; Dolphin, D. *J. Org. Chem.* **2009**, *74*, 5237−5243.

(8) (a) Li, H.; Nguyen, N.; Fronczek, F. R.; Vicente, M. G. H. *Tetrahedron* **2009**, *65*, 3357−3363. (b) Matsushita, O.; Derkacheva, V. M.; Muranaka, A.; Shimizu, S.; Uchiyama, M.; Luk'yanets, E. A.; Kobayashi, N. *J. Am. Chem. Soc.* **2012**, *134*, 3411−3418.

(9) (a) Li, J.; Zhang, K.; Zhang, X.; Huang, K.-W.; Chi, C.; Wu, J. *J. Org. Chem.* **2010**, *75*, 856−863. (b) Li, J.; Jiao, C.; Huang, K.-W.; Wu, J. *Chem. - Eur. J.* **2011**, *17*, 14672−14680.

(10) (a) Loudet, A.; Burgess, K. *Chem. Rev.* **2007**, *107*, 4891−4932. (b) Ulrich, G.; Ziessel, R.; Harriman, A. *Angew. Chem., Int. Ed.* **2008**, *47*, 1184−1201. (c) Benstead, M.; Mehl, G. H.; Boyle, R. W. *Tetrahedron* **2011**, *67*, 3573−3601. (d) Bessette, A.; Hanan, G. S. *Chem. Soc. Rev.* **2014**, *43*, 3342−3405. (e) Singh, S. P.; Gayathri, T. *Eur. J. Org. Chem.* **2014**, *2014*, 4689−4707.

(11) (a) Ni, Y.; Wu, J. *Org. Biomol. Chem.* **2014**, *12*, 3774−3791. (b) Wu, Y.; Cheng, C.; Jiao, L.; Yu, C.; Wang, S.; Wei, Y.; Mu, X.; Hao, E. *Org. Lett.* **2014**, *16*, 748−751. (c) Jiang, X.-D.; Xi, D.; Zhao, J.; Yu, H.; Sun, G.-T.; Xiao, L.-J. *RSC Adv.* **2014**, *4*, 60970−60973. (d) Ertem, E.; Bekdemir, A.; Atilgan, A.; Akkaya, E. U. *Pure Appl. Chem.* **2014**, *86*, 899−903. (e) Jiang, X.-D.; Xi, D.; Sun, C.-l.; Guan, J.; He, M.; Xiao, L.-J. *Tetrahedron Lett.* **2015**, *56*, 4868−4870.

DOI: 10.1021/acs.joc.5b02720
J. Org. Chem. 2016, 81, 1310−1315

(12) Kang, H. C.; Haugland, R. P. U. S. Patent 5,433,896, July 18, 1995.
(13) (a) Wada, M.; Ito, S.; Uno, H.; Murashima, T.; Ono, N.; Urano, T.; Urano, Y. *Tetrahedron Lett.* **2001**, *42*, 6711−6713. (b) Shen, Z.; Röhr, H.; Rurack, K.; Uno, H.; Spieles, M.; Schulz, B.; Reck, G.; Ono, N. *Chem. - Eur. J.* **2004**, *10*, 4853−4871. (c) Goeb, S.; Ziessel, R. *Org. Lett.* **2007**, *9*, 737−740. (d) Goeb, S.; Ziessel, R. *Tetrahedron Lett.* **2008**, *49*, 2569−2574. (e) Ulrich, G.; Goeb, S.; De Nicola, A.; Retailleau, P.; Ziessel, R. *J. Org. Chem.* **2011**, *76*, 4489−4505. (f) Suda, Y.; Nishiyabu, R.; Kubo, Y. *Tetrahedron* **2015**, *71*, 4174−4182.
(14) (a) Kubo, Y.; Minowa, Y.; Shoda, T.; Takeshita, K. *Tetrahedron Lett.* **2010**, *51*, 1600−1602. (b) Tomimori, Y.; Okujima, T.; Yano, T.; Mori, S.; Ono, N.; Yamada, H.; Uno, H. *Tetrahedron* **2011**, *67*, 3187−3193. (c) Kubo, Y.; Watanabe, K.; Nishiyabu, R.; Hata, R.; Murakami, A.; Shoda, T.; Ota, H. *Org. Lett.* **2011**, *13*, 4574−4577.
(15) (a) Umezawa, K.; Nakamura, Y.; Makino, H.; Citterio, D.; Suzuki, K. *J. Am. Chem. Soc.* **2008**, *130*, 1550−1551. (b) Umezawa, K.; Matsui, A.; Nakamura, Y.; Citterio, D.; Suzuki, K. *Chem. - Eur. J.* **2009**, *15*, 1096−1106.
(16) (a) Awuah, S. G.; Polreis, J.; Biradar, V.; You, Y. *Org. Lett.* **2011**, *13*, 3884−3887. (b) Yang, Y.; Guo, Q.; Chen, H.; Zhou, Z.; Guo, Z.; Shen, Z. *Chem. Commun.* **2013**, *49*, 3940−3942. (c) Awuah, S. G.; Das, S. K.; D'Souza, F.; You, Y. *Chem. - Asian J.* **2013**, *8*, 3123−3132.
(17) (a) Jiao, C.; Huang, K.-W.; Wu, J. *Org. Lett.* **2011**, *13*, 632−635. (b) Zeng, L.; Jiao, C.; Huang, X.; Huang, K.-W.; Chin, W.-S.; Wu, J. *Org. Lett.* **2011**, *13*, 6026−6029.
(18) Hayashi, Y.; Obata, N.; Tamaru, M.; Yamaguchi, S.; Matsuo, Y.; Saeki, A.; Seki, S.; Kureishi, Y.; Saito, S.; Yamaguchi, S.; Shinokubo, H. *Org. Lett.* **2012**, *14*, 866−869.
(19) Sarma, T.; Panda, P. K.; Setsune, J. *Chem. Commun.* **2013**, *49*, 9806−9808.
(20) Okujima, T.; Shida, Y.; Ohara, K.; Tomimori, Y.; Nishioka, M.; Mori, S.; Nakae, T.; Uno, H. *J. Porphyrins Phthalocyanines* **2014**, *18*, 752−761.
(21) (a) Nakamura, M.; Tahara, H.; Takahashi, K.; Nagata, T.; Uoyama, H.; Kuzuhara, D.; Mori, S.; Okujima, T.; Yamada, H.; Uno, H. *Org. Biomol. Chem.* **2012**, *10*, 6840−6849. (b) Wakamiya, A.; Murakami, T.; Yamaguchi, S. *Chem. Sci.* **2013**, *4*, 1002−1007. (c) Nakamura, M.; Kitatsuka, M.; Takahashi, K.; Nagata, T.; Mori, S.; Kuzuhara, D.; Okujima, T.; Yamada, H.; Nakae, T.; Uno, H. *Org. Biomol. Chem.* **2014**, *12*, 1309−1317. (d) Yu, C.; Jiao, L.; Li, T.; Wu, Q.; Miao, W.; Wang, J.; Wei, Y.; Mu, X.; Hao, E. *Chem. Commun.* **2015**, *51*, 16852−16855.
(22) Zhou, X.; Wu, Q.; Feng, Y.; Yu, Y.; Yu, C.; Hao, E.; Wei, Y.; Mu, X.; Jiao, L. *Chem. - Asian J.* **2015**, *10*, 1979−1986.
(23) Lu, H.; Shimizu, S.; Mack, J.; Shen, Z.; Kobayashi, N. *Chem. - Asian J.* **2011**, *6*, 1026−1037.
(24) Sharma, S.; Kim, A.; Park, J.; Kim, M.; Kwak, J. H.; Jung, Y. H.; Park, J. S.; Kim, I. S. *Org. Biomol. Chem.* **2013**, *11*, 7869−7876.
(25) Knight, J. D.; Brown, J. B.; Overby, J. S.; Beam, C. F.; Camper, N. D. *J. Heterocycl. Chem.* **2008**, *45*, 189−194.
(26) (a) Bellier, Q.; Dalier, F.; Jeanneau, E.; Maury, O.; Andraud, C. *New J. Chem.* **2012**, *36*, 768−773. (b) Chen, J.; Reibenspies, J.; Derecskei-Kovacs, A.; Burgess, K. *Chem. Commun.* **1999**, 2501−2502. (c) Bellier, Q.; Pégaz, S.; Aronica, C.; Guennic, B. L.; Andraud, C.; Maury, O. *Org. Lett.* **2011**, *13*, 22−25.
(27) Lakowicz, R. *Principles of Fluorescence Spectroscopy*; Kluwer: New York, 1999.
(28) Pommerehne, J.; Vestweber, H.; Guss, W.; Mahrt, R. F.; Bässler, H.; Porsch, M.; Daub, J. *Adv. Mater.* **1995**, *7*, 551−554.
(29) Xu, H.; Wada, T.; Ohkita, H.; Benten, H.; Ito, S. *Sci. Rep.* **2015**, *5*, 9321.
(30) Sheldrick, G. M. *Acta Crystallogr., Sect. A: Found. Crystallogr.* **2008**, *A64*, 112−122.
(31) Crosby, G. A.; Demas, J. N. *J. Phys. Chem.* **1971**, *75*, 991−1024.
(32) Berezin, M. Y.; Guo, K.; Akers, W.; Northdurft, R. E.; Culver, J. P.; Teng, B.; Vasalatiy, O.; Barbacow, K.; Gandjbakhche, A.; Griffiths, G. L.; Achilefu, S. *Biophys. J.* **2011**, *100*, 2063−2072.
(33) Frisch, M. J.; Trucks, G. W.; Schlegel, H. B.; Scuseria, G. E.; Robb, M. A.; Cheeseman, J. R.; Scalmani, G.; Barone, V.; Mennucci, B.; Petersson, G. A.; Nakatsuji, H.; Caricato, M.; Li, X.; Hratchian, H. P.; Izmaylov, A. F.; Bloino, J.; Zheng, G.; Sonnenberg, J. L.; Hada, M.; Ehara, M.; Toyota, K.; Fukuda, R.; Hasegawa, J.; Ishida, M.; Nakajima, T.; Honda, Y.; Kitao, O.; Nakai, H.; Vreven, T.; Montgomery, J. A., Jr.; Peralta, J. E.; Ogliaro, F.; Bearpark, M.; Heyd, J. J.; Brothers, E.; Kudin, K. N.; Staroverov, V. N.; Keith, T.; Kobayashi, R.; Normand, J.; Raghavachari, K.; Rendell, A.; Burant, J. C.; Iyengar, S. S.; Tomasi, J.; Cossi, M.; Rega, N.; Millam, J. M.; Klene, M.; Knox, J. E.; Cross, J. B.; Bakken, V.; Adamo, C.; Jaramillo, J.; Gomperts, R.; Stratmann, R. E.; Yazyev, O.; Austin, A. J.; Cammi, R.; Pomelli, C.; Ochterski, J. W.; Martin, R. L.; Morokuma, K.; Zakrzewski, V. G.; Voth, G. A.; Salvador, P.; Dannenberg, J. J.; Dapprich, S.; Daniels, A. D.; Farkas, Ö.; Foresman, J. B.; Ortiz, J. V.; Cioslowski, J.; Fox, D. J. *Gaussian 09*, revision C.01; Gaussian, Inc.: Wallingford, CT, 2010.

DOI: 10.1021/acs.joc.5b02720
J. Org. Chem. 2016, 81, 1310−1315